





Iron impact on the quality of sand casting made from secondary AlSi7Mg0.6 alloy used in the automotive and aerospace industry

Lucia Pastierovičová¹✉, Lenka Kuchariková², Eva Tillová³, Mária Chalupová⁴

¹  <https://orcid.org/0000-0001-5341-9292>

²  <https://orcid.org/0000-0002-2688-1075>

³  <https://orcid.org/0000-0002-1010-0713>

⁴  <https://orcid.org/0000-0003-0175-9484>

University of Žilina, Faculty of Mechanical Engineering, Department of Materials Engineering
Univerzitná 8215/1, 010 26 Žilina, Slovak Republic
e-mail: {¹lucia.pastierovicova; ²lenka.kucharikova; ³eva.tillova; ⁴maria.chalupova@fstroj.uniza.sk}
✉ corresponding author

Keywords: the casting quality, secondary aluminum, aluminum alloys, Fe content, porosity, automotive

JEL Classification: L15, L61, L62

Abstract

Due to the high demand for secondary alloys in the automotive and aerospace industry, this work investigates the effect of higher iron content on the quality of AlSi7Mg0.6 sand castings. Secondary-recycled Al-Si alloys contain an increased amount of impurities due to their remelting of scrap metal. One of the most unwanted impurities found in these alloys is iron. Iron leads to the formation of various Fe-rich intermetallic phases, whose morphology influences the mechanical properties even at low Fe content. It also promotes the formation of casting defects, such as porosity and shrinkage. The formation of porosity in secondary Al-alloys is another major aspect that can affect the final properties of castings. Since these materials are mainly used to produce castings for the automotive industry, such as engine blocks, cylinder heads, and so on, it is necessary to produce castings without any defects. Therefore, the quality of AlSi7Mg0.6 sand casting is investigated at lower iron content (0.128% wt. Fe) and compared to the higher iron content (0.429% wt. Fe), whereby a correlation between iron content and porosity is monitored.

Introduction

Nowadays, the automotive industry has a key role in the economy of developed countries. Regarding the latest trends in automobile manufacturing, the main priority is to implement the principles of lightweight construction to meet customer demands, reduce gas emissions and fuel consumption, and optimize mechanical performance. For these reasons, it is necessary to perfectly match the choice of materials to the operating life of the components (Tisza & Czinege, 2018; Bogdanoff et al., 2021).

The environmental and economic advantages of secondary-recycled aluminum alloys make them the best candidate materials for various applications in different industries, such as automotive, construction, aerospace, etc. Secondary Al-alloys are made from aluminum scrap and recyclable aluminum waste by recycling. Aluminum can be recycled repeatedly without loss of its properties. The high value of aluminum scrap is a major incentive and economic impetus for recycling. Remelting the Al-recycled material saves almost 95% of the energy consumption required to produce primary-ore

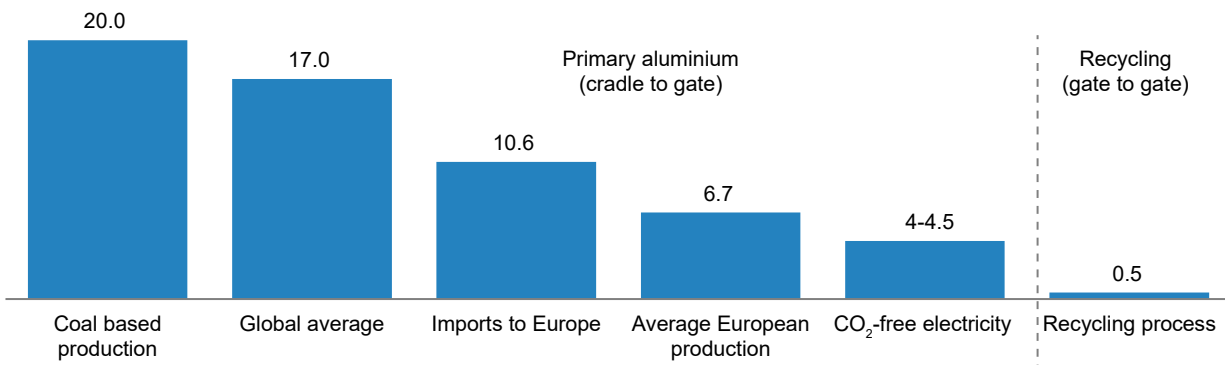
Tonne of CO₂-eq/tonne of production

Figure 1. Greenhouse gas emissions of primary aluminum production and recycling process (World Aluminum, 2015)

aluminum, thus avoiding corresponding emissions, including greenhouse gases as depicted in Figure 1 (Song et al., 2022; Tillová, Chalupová & Kuchariková 2012).

Al-Si-based alloys are the most widely used types of foundry Al-alloys. The quality of secondary Al-Si alloys is considered a key factor in alloy selection casting for a specific engineering application. Due to lightweight, fluidity, castability, fabricability, high strength-to-weight ratio, low density, good corrosion resistance, etc., castings from secondary Al-alloys have applications in a wide range of industries. However, their use in the transport sector has become increasingly rapid (Figure 2). Heat-treatable Al-Si-Mg alloys, in particular, are widely used to produce automotive castings such as cylinder blocks, steering knuckles, cylinder heads, valve lifters, pistons, and so on (Tillová, Chalupová & Kuchariková, 2012; Svobodova, Lunak & Lattner, 2019; Kuchariková et al., 2020; Abdelaziz et al., 2022; Li et al., 2022).

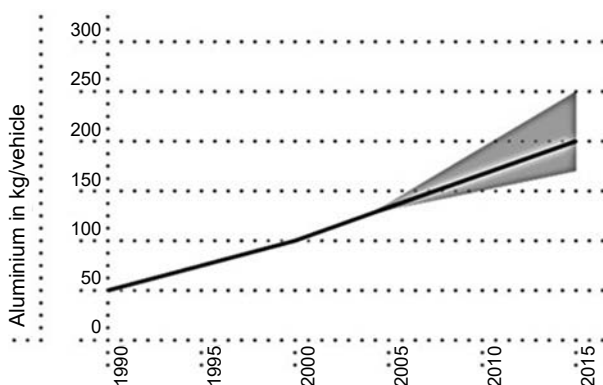


Figure 2. Aluminum content in European vehicles (EAA/OEA, 2006)

Improving the mechanical properties and structure of Al-alloys can increase the life of the casting.

To achieve optimal mechanical properties, various elements such as Ni, Mg, Cr, Mn, and Zn are added to the melt. However, the unavoidable elements that act as impurities seriously reduce the complex mechanical properties of secondary Al-alloys. A significant problem with many of the unavoidable co-elements is the complicated process of eliminating their negative effects on Al-Si-Mg alloys. In most cases, they cannot be removed under foundry conditions. Therefore, their content needs to be reduced to an acceptable limit (Farkašová, Tillová & Chalupová, 2013; Bacaicoa et al., 2019; Song et al., 2022).

Due to the increasing production of secondary Al-castings, it is necessary to ensure strict metallurgical quality control (Farkašová, Tillová & Chalupová, 2013; Hirsch et al., 2022). This is because the quality of this casting is influenced by the higher presence of Fe. The recycling process leads to an accumulation of Fe from impurities in bauxite ore and from contamination of scrap aluminum by ferrous metal. Fe cannot be easily removed from the melt by conventional foundry treatment; only dilution seems to be practical, via an uneconomical method to reduce its Fe content in the alloy. Fe is also the most harmful impurity in recycled Al-Si alloys with low solubility in Al-alloys, formed as an intermetallic phase. Among the Fe-rich phases, the most significant in Al-Si-Mg alloys are the β -Al₅FeSi (β -Fe) and α -Al₁₅(FeMg)₃Si₂ (α -Fe) phases. The β -Fe phase is very harmful due to its three-dimensional platelets or fragile two-dimensional needle-like morphology. It is well-known that the presence of the Fe-phase affects the increased formation of porosity and shrinkage due to the large Fe-needles preventing the melt flow, which causes the presence of shrinkage pores. In addition, the investigation by Brueckner-Foit et al. (Brueckner-Foit et al., 2017) proved the damage mechanism in a secondary alloy of shrinkage pores, found on the

inner side of the specimen, acted as primary crack initiation sites.

Many authors reviewed techniques to neutralize the detrimental effects of Fe by the addition of elements such as Mn, Co, Cr, Be, and Sr. Mn is a widely used element to remove the harmful Al_5FeSi phase. Mn addition of up to half the amount of Fe leads to the formation of a less harmful shape $\alpha\text{-(Al}_{15}\text{(Fe,Mn)}_3\text{Si}_2)$, with a skeleton-like or Chinese-script-like morphology that does not initiate cracks (Taylor, Caceres & Crepel, 2008; Bacaicoa et al., 2019; Svobodova, Lunak & Lattner, 2019; Tillová et al., 2019; Song et al., 2022).

Unfortunately, Al-Si-Mg alloys are susceptible to extensive porosity, not only for higher Fe content but also due to the decreasing solidification rates in sand molds. Unlike alloys cast into metal molds that quickly solidify and refine dendritic cells owing to their excellent ability to transfer heat. Another disadvantage of sand molds is that castings made in metal molds are usually more ductile than those made in sand molds (Mae et al., 2008; Kasala et al., 2011; Davor, Špada & Ilkic, 2019; Fiocchi, Biffi & Tuissi, 2020; Reyes et al., 2020).

Since a high amount of Fe can negatively affect the quality of aluminum castings by forming porosity, it is imperative to minimize its content and, thus, reduce its negative impact because porosity is still the most critical problem. Therefore, this study investigates the quality of AlSi7Mg0.6 sand casting with a consideration of structural defects caused by different Fe content.

Experimental material and procedures

An experimental material was used: secondary AlSi7Mg0.6 (EN AC 42 200, A357) cast alloy produced by Uneko Ltd., Czech Republic. Three alloys were cast with different Fe content: A (0.128% wt. Fe) and B, C (0.429% wt. Fe). The addition of Mn (0.149 wt. %) was intentionally added to alloy C in the form of a pre-alloy AlMn75, with the aim of investigating the Mn effect on structural components. From the alloys (A, B, C) were cast experimental bars with dimensions $\phi 20$ mm and length of 300 mm, into sand molds by a gravity casting method. The casting temperature was 750°C, and the refining temperature was 740–745°C. The ECOSAL AL 113S salt was used as a refining salt. Experimental bars were heat-treated according to the T6 method. The heat treatment of T6 was carried out at UNEKO, s.r.o. and consisted of a dissolution annealing at 530°C \pm 5°C with a holding time of 7 hours.

Rapid cooling to 50°C was then followed by artificial aging at 160 °C for 6 hours. The chemical composition of the experimental alloys, according to the delivery list, is shown in Table 1.

Table 1. Chemical composition of AlSi7Mg0.6 alloys [wt. %]

Alloy	Si	Fe	Cu	Mn	Mg	Ti
A	6.742	0.128	0.012	0.046	0.519	0.108
B	7.097	0.429	0.013	0.044	0.466	0.119
C	6.881	0.429	0.011	0.149	0.596	0.103

In alloys: Ni (< 0.002), Cr (< 0.002), Pb (< 0.005), Sn (< 0.003), Na (< 0.006), Sr (< 0.002), Al (rest)

The experimental alloy AlSi7Mg0.6 is commonly heat-treated to improve its strength properties. After heat treatment, it becomes one of the strongest sand-cast secondary Al-Si-Mg alloys, widely used to produce frames, brackets, housings, and other automobile parts.

Samples used for metallographic evaluation were cut from the experimental bars using an MTH MICRON 3000 automatic saw with water cooling applied to avoid heating effects and deformation of the microstructure. After the cutting, the samples were prepared by standard metallographic procedures (wet-ground on SiC papers, polished by a Struers Op-S, and etched by 0.5% HF and 95% H₂SO₄ to highlight the Fe-rich phases). After each operation, the samples were rinsed with warm water, ethanol, and then dried with hot air.

Prepared samples were observed by using an optical microscope Neophot 32 and a scanning electron microscope (SEM) VEGA LMU II. A quantitative analysis was performed by using the image analyzer NIS Elements 4.0 to numerically evaluate porosity and the size of the pores. The resulting average values were calculated from a minimum of 15 measurements.

Results and discussion

The representative microstructures of experimental A, B, and C alloys are shown in Figure 3, which corresponds to the typical hypoeutectic microstructure consisting of primary α -Al dendrites, eutectic (mixture of α -matrix and spherical grey Si-particles), and intermetallic Fe- and Mg-rich phases, primarily concentrated in the inter-dendritic areas. The needle-like Al_5FeSi phase was present.

Increased Fe content leads to the formation of longer Fe phases in the form of plates/needles in alloy B compared to alloy A. Therefore, it is confirmed that, with increasing Fe content, the presence

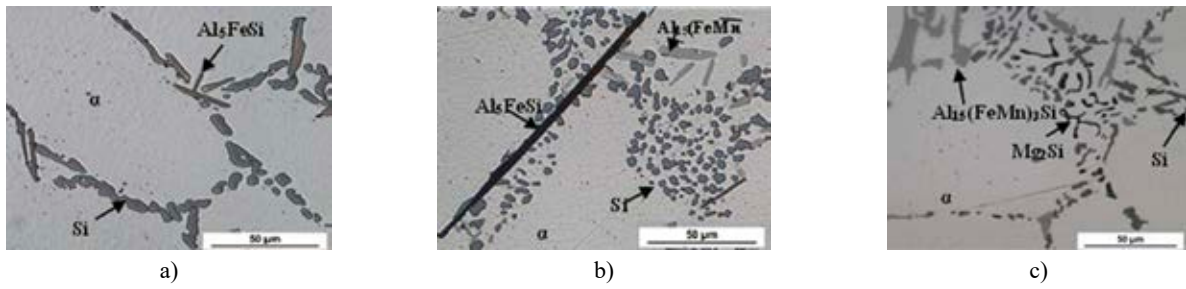


Figure 3. Microstructure of AlSi7Mg0.6, etch. 0.5% HF: a) alloy A, b) alloy B, and c) alloy C

of Fe needles and their length ascend as well. With the increased amount of Mg in alloy C, it was possible to also observe the intermetallic phase Mg_2Si intermetallic phase in the form of fine spheroidized black particles (depicted in Figure 3c). From Figure 3, it can be proved that the addition of Mn into alloy C has a positive effect on the transformation of needle-like Al_5FeSi into a less harmful skeletal $Al_{15}(FeMn)_3Si_2$ intermetallic phase. Additionally, it can be observed that the heat treatment led to the spheroidization of the eutectic silicon, which is not in the form of plates (Kucharikova, Tillová & Chalupová, 2016) but in the form of spheroidized particles (Figure 3).

From the average porosity results in Table 2, for alloy C, in which Mn was intentionally added, the area fraction of the pores was the largest. The largest average pore sizes were also measured in alloy C. The smallest average pore sizes were in alloy A, with the lowest Fe content, and their size increased with a growth in the Fe content. These results correlate with the research of Taylor et al. (Taylor, Caceres & Crepel, 2008), who investigated the effect of Mn

in a higher Fe-alloy on the porosity of castings; they concluded that the presence of Mn does not guarantee an improvement in the porosity. Manganese appears to reduce the higher amount of porosity associated with an increased Fe content, primarily in Cu-containing Al-Si alloys or at the correct $Fe/Mn = 2/1 = 0.5$ ratios (Table 2). Increased porosity in alloy C (Table 2), with the addition of Mn, is possibly related to the low Mn content added to the correction of the β -phase, displayed in Table 1.

The evaluation of the porosity and pore sizes show that the pores are in close contact with the Al_5FeSi needles, shown in Figure 4. This pore formation confirmed the investigations of Puncreobutr et al. (Puncreobutr et al., 2014) and Brueckner-Foit et al. (Brueckner-Foit et al., 2017) that Fe-needles

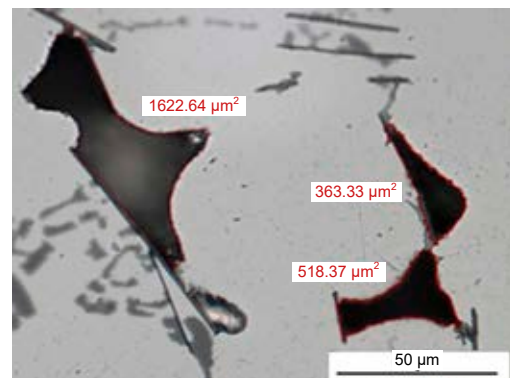


Figure 4. Pore formation surrounding the Al_5FeSi needles in an AlSi7Mg0.6 alloy B, etch. H_2SO_4

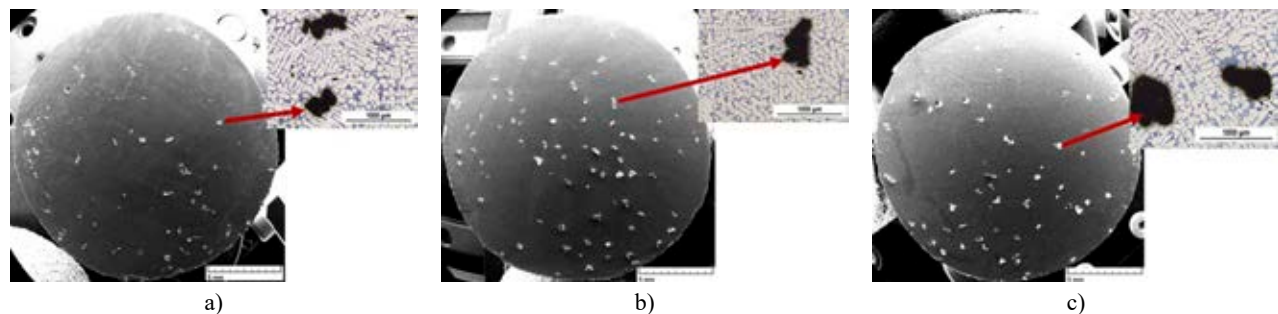


Figure 5. Macrographs of the cross-section of the AlSi7Mg0.6 alloys etch. 0.5% HF: a) alloy A, b) alloy B, and c) alloy C

are surrounded by pores and act as nucleation sites for porosity. Therefore, the alloy with the highest content of Fe (i.e., alloy C) has the highest porosity.

The SEM surface macrographs are in Figure 5; it shows the distribution of the pores of the investigated alloys. The porosity in the experimental alloys A, B, and C was observed to be directly proportional to the % Fe. In alloy A, with 0.128 wt.% Fe (Figure 5a), sponge-shaped pores were observed mainly in the center of the casting. For alloys B and C with 0.429 wt.% Fe, the pores appeared to be distributed over a larger area (Figure 5b, c) and locally large pores are found at the edge of the casting.

Summary and conclusion

The results of the quantitative analysis proved the impact of iron on the quality of sand castings from AlSi7Mg0.6 alloy as follows:

- The quality of experimental alloys is significantly affected by Fe-rich phases, which promote the formation of casting defects such as shrinkage pores.
- In experimental alloys A, B, and C, mainly Fe-rich intermetallic phases were present, the needle-like β -Al₃FeSi. Another type of Fe-rich phase, skeletal, or Chinese script-like α -Al₁₅(FeMn)₃Si₂ phase was also present in alloys B and C. In all the alloys, the Mg₂Si phase was identified in the form of fine spherical particles.
- With increasing Fe content, both the porosity and the average pore size grow, most of the pores being surrounded by Fe-rich phases.
- The addition of Mn positively affects the transformation of needle-like β -Al₃FeSi to skeletal α -Al₁₅(FeMn)₃Si₂. On the other hand, Mn negatively affects the porosity in alloy C (0.429 wt.% Fe). With the addition of 0.149 wt.% Mn, both the porosity and the average pore size significantly increased, probably due to the low Mn content added for the correction of the β -Al₃FeSi.

Acknowledgments

The research was supported by the Scientific Grand Agency of the Ministry of Education of Slovak Republic and Slovak Academy of Sciences, VEGA 01/0398/19, KEGA 016ŽU-4/2020, and project to support young researchers at UNIZA, ID of project 12715 – project leader Ing. Lenka Kuchariková. This article was also funded by the University of Žilina project 313011ASY4: “Strategic implementation of additive technologies to strengthen the

intervention capacities of emergencies caused by the COVID-19 pandemic”.

References

1. ABDELAZIZ, M.H., SAMUEL, A.M., DOTY, H.W., SONGMENE, V. & SAMUEL, F.H. (2022) Mechanical performance and precipitation behavior in Al-Si-Cu-Mg cast alloys: Effect of prolonged thermal exposure. *Materials* 15(8), 2830.
2. BACAICOA, I., LUETJE, M., ZEISMANN, F., GEISERT, A., FEHLBIER, M. & BRUECKNER-FOIT, A. (2019) On the role of Fe-content on the damage behavior of an Al-Si-Cu alloy. *Procedia Structural Integrity* 23, pp. 33–38.
3. BOGDANOFF, T., LATTANZI, L., MERLIN, M., GHASSEMALI, E., JARFORS, A.E.W. & SEIFEDDINE, S. (2021) The complex interaction between microstructural features and crack evolution during cyclic testing in heat-treated Al-Si-Mg-Cu cast alloys. *Materials Science and Engineering: A* 825, 141930.
4. BRUECKNER-FOIT, A., LUETJE, M., BACAICOA, I., GEISERT, A. & FEHLBIER, M. (2017) On the role of internal defects in the fatigue damage process of a cast Al-Si-Cu alloy. *Procedia Structural Integrity* 7, pp. 36-43, doi: 10.1016/j.prostr.2017.11.058.
5. DAVOR, S., ŠPADA, V. & ILKIC, D. (2019) Influence of natural aging on the mechanical properties of high pressure die casting (HPDC) EN AC 46000-ALSi9Cu3(Fe) Al alloy. *Materials Testing* 61(5), pp. 448–454.
6. EAA/OEA (2006) *Aluminum Recycling in Europe*. [Online]. Available from: brochure available online https://recycling.world-aluminium.org/fileadmin/_migrated/content_uploads/f10000217_04.pdf [Accessed: October 21, 2022].
7. FARKAŠOVÁ, M., TILLOVÁ, E. & CHALUPOVÁ, M. (2013) Fracture surface of recycled AlSi10Mg cast alloy. *Manufacturing Technology* 13(3), pp. 307–313.
8. FIOCHCI, J., BIFFI, C.A. & TUISSI, A. (2020) Selective laser melting of high-strength primary AlSi9Cu3 alloy: Processability, microstructure, and mechanical properties. *Materials & Design* 191, 108581.
9. HIRSCH, S.J., WINTER, L., GRUND, T. & LAMPKE, T. (2022) Heat treatment influencing porosity and tensile properties of field assisted sintered AlSi7Mg0.6. *Materials* 15(7), 2503.
10. KASALA, J., PERNIS, R., PERNIS, I. & LIČKOVÁ, M. (2011) Influence of iron and manganese quality on pore level in the Al-Si-Cu. *Chem. Letters* 105, pp. 627–629 [in Slovak].
11. KUCHARIKOVÁ, L., TILLOVÁ, E. & CHALUPOVÁ, M. (2016) The Si particles morphology in hypoeutectic Al-Si casts. *Materials Today: Proceedings* 3(4), pp. 1031–1036.
12. KUCHARIKOVÁ, L., TILLOVÁ, E., CHALUPOVÁ, M. & HANUSOVÁ, P. (2020) Investigation on microstructural and hardness evaluation in heat-treated and as-cast state of secondary AlSiMg cast alloys. *Materials Today: Proceedings* 32, Part 2, pp. 63–67.
13. LI, Y., HU, A., FU, Y., LIU, S., SHEN, W., HU, H. & NIE, X. (2022) Al alloys and casting processes for induction motor applications in battery-powered electric vehicles: A review. *Metals* 12(2), 216.
14. MAE, H., TENG, X., BAI, Y. & WIERZBICKI, T. (2008) Comparison of ductile fracture properties of aluminum castings: Sand mold vs. metal mold. *International Journal of Solids and Structures* 45(5), pp. 1430–1444.
15. PUNCREOBUTR, C., LEE, P.D., KAREH, K.M., CONNOLLEY, T., FIFE, J.L. & PHILLION, A.B. (2014) Influence of Fe-rich intermetallics on solidification defects in Al-Si-Cu alloys. *Acta Materialia* 68, pp. 42–51.

16. REYES, A.E.S., GUERRERO, G.A., ORTIZ, G.R., GASGA, J.R., ROBLEDO, J.F.G., FLORES, O.L. & COSTA, P.S. (2020) Microstructural, microscratch and nanohardness mechanical characterization of secondary commercial HPDC AlSi9Cu3-type alloy. *Journal of Materials Research and Technology* 9(4), pp. 8266–8282.
17. SONG, D.-F., ZHAO, Y.-L., WANG, Z., JIA, Y.-W., LI, D.-X., FU, Y.-N., ZHANG, D.-T. & ZHANG, W.-W. (2022) 3D Fe-rich phases evolution and its effects on the fracture behavior of Al-7.0Si-1.2Fe alloys by Mn neutralization. *Acta Metallurgica Sinica (English Letters)* 35(1), pp. 163–175.
18. SVOBODOVA, J., LUNAK, M. & LATTNER, M. (2019) Analysis of the increased iron content on the corrosion resistance of the AlSi7Mg0.3 alloy casting. *Manufacturing Technology* 19(6), pp. 1041–1046.
19. TAYLOR, J.A., CACERES, C.H. & CREPEL, L. (2008) *The effect of Si and Cu content on Fe-containing intermetallic particles in Al-Si-Cu0.8Fe alloys*. 11th International Conference of Aluminium Alloys (ICAA11), 22–26 September 2008, Aachen, Germany, pp. 105–114.
20. TILLOVÁ, E., CHALUPOVÁ, M. & KUCHARIKOVÁ, L. (2012) Evolution of phases in a recycled Al-Si cast alloy during solution treatment. In: Kazmiruk, V. (ed.) *Scanning Electron Microscopy*, doi: 10.5772/34542.
21. TILLOVÁ, E., CHALUPOVÁ, M., KUCHARIKOVÁ, L., ŠVECŮVÁ, I. & BELAN, J. (2019) Sludge phases as a cause of higher wear of cutting tools during machining of secondary AlSi12Cu1 castings. *Manufacturing Technology* 19(5), pp. 874–879.
22. TISZA, M. & CZINEGE, I. (2018) Comparative study of the application of steels and aluminum in lightweight production of automotive parts. *International Journal of Lightweight Materials and Manufacture* 1(4), pp. 229–238.
23. World Aluminum (2015) Coal-based production and global average: Life cycle inventory data and environmental metrics for the primary aluminum industry. [Online]. Available from: <https://fluoridealert.org/wp-content/uploads/aluminum.life-cycle.2015.pdf> [Accessed: October 21, 2022].

Cite as: Pastierovičová, L., Kuchariková, L., Tillová, E., Chalupová, M. (2022) Iron impact on the quality of sand casting made from secondary AlSi7Mg0.6 alloy used in the automotive and aerospace industry. *Scientific Journals of the Maritime University of Szczecin, Zeszyty Naukowe Akademii Morskiej w Szczecinie* 72 (144), 86–91.